Lipid nanoparticle formulated protein transduction domain-bone morphogenetic protein-2 enhances wound healing in type 1 diabetic mice

Jae Wan Suh

Department of Medicine

The Graduate School, Yonsei University

Lipid nanoparticle formulated protein transduction domain-bone morphogenetic protein-2 enhances wound healing in type 1 diabetic mice

Directed by Professor Jin Woo Lee

The Doctoral Dissertation
submitted to the Department of Medicine,
the Graduate School of Yonsei University
in partial fulfillment of the requirements for the degree
of Doctor of Philosophy

Jae Wan Suh

June 2022

This certifies that the Doctoral Dissertation of Jae Wan Suh is approved.

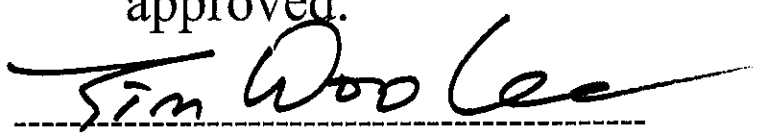

Thesis Supervisor: Jin Woo Lee

Thesis Committee Member#1: Won Jai Lee

Thesis Committee Member#2: Jong In Yook

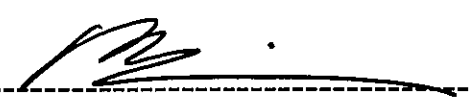

Thesis Committee Member#3: Dae-Won Kim

Thesis Committee Member#4: Kwang Hwan Park

The Graduate School
Yonsei University

June 2022

ACKNOWLEDGEMENTS

I would like to express my sincere gratitude to my advisor, Professor Jin Woo Lee, for his unwavering encouragement and support. His guidance, which has emphasized excellence, helped me immensely as I researched and wrote my thesis.

I would also like to thank the rest of my thesis committee, Professors Jong In Yook, Won Jai Lee, Dae-Won Kim, and Kwang Hwan Park, for their encouragement and insightful comments. The assistance provided by Dr. Kyoung-Mi Lee and colleagues in the laboratory is also greatly appreciated.

I especially thank my parents for praying for me and Samuel and Bo Hyon for their support while I completed my thesis.

<TABLE OF CONTENTS>

LIST OF FIGURES

ABSTRACT

Lipid nanoparticle formulated protein transduction domain-bone morphogenetic protein-2 enhances wound healing in type 1 diabetic mice

Jae Wan Suh

Department of Medicine

The Graduate School, Yonsei University

(Directed by Professor Jin Woo Lee)

Decreased angiogenesis contributes to delayed wound healing in diabetic patients. Recombinant human bone morphogenetic protein-2 (rhBMP2), which has been approved by the FDA for inducing bone regeneration, has also been shown to promote angiogenesis. However, the short half-lives of soluble growth factors such as rhBMP2 limit their use in wound-healing applications. To overcome this limitation, we propose a novel delivery model utilizing a protein transduction domain (PTD) formulated in lipid nanoparticle (LNP). We aim to determine whether a gelatin hydrogel dressing loaded with LNP formulated PTD-BMP2 (LNP-PTD-BMP2) can improve the angiogenic function of BMP2 and improve diabetic wound healing. In vitro, we found that compared to the control and rhBMP2, LNP-PTD-BMP2 induced higher tube formation of human umbilical vein endothelial cells and increased the cell recruitment capacity of HaCaT cells

in a scratch wound assay. Large, full-thickness back skin wounds were inflicted on streptozotocin-induced diabetic mice. Gelatin hydrogel cross-linked by microbial transglutaminase containing rhBMP2, LNP-PTD-BMP2, or a control was applied to diabetic wounds. Wounds treated with LNP-PTD-BMP2 exhibited enhanced wound closure, increased re-epithelialization rates, and higher collagen deposition than the rhBMP2 or control treatments. In an immunofluorescence study, the LNP-PTD-BMP2 treatment showed more CD31- and α-SMA-positive cells, thus demonstrating a higher neovascularization capacity than rhBMP2 or control treatments. Additionally, *in vivo* near-infrared fluorescent images showed that LNP-PTD-BMP2 has a longer half-life than rhBMP2 and that BMP2 localizes around wounds. These findings suggest that LNP-PTD-BMP2-loaded gelatin hydrogel is a viable treatment for diabetic wounds.

Key words: diabetes, wound healing, angiogenesis, lipid nanoparticle, protein transduction domain, bone morphogenetic protein-2, gelatin hydrogel

Lipid nanoparticle formulated protein transduction domain-bone morphogenetic protein-2 enhances wound healing in type 1 diabetic mice

Jae Wan Suh

Department of Medicine
The Graduate School, Yonsei University

(Directed by Professor Jin Woo Lee)

I. INTRODUCTION

Diabetes mellitus is a chronic metabolic disorder that affects millions of people worldwide.[1,2] Diabetic foot ulceration is one of the most common complications of diabetes and is associated with delayed wound healing.[3,4] In wound healing, the stages of inflammation, cell migration and proliferation, and tissue remodeling proceed in a well-coordinated sequence of cellular and biomolecular events.[2,5] However, in diabetic wounds, chemokine production and inflammatory responses are abnormal, growth factor levels are decreased, and angiogenic ability is reduced.[4,6-8] Previous research has investigated the efficacy of advanced treatments such as stem cells, chemokines, growth factors, skin substitutes, and gene therapy for improving diabetic wound healing. However, the efficacy of these treatments is low, necessitating the development of more effective treatment methods.[9]

Insufficient angiogenesis leads to limited recruitment of inflammatory cells and reduced supply of oxygen and nutrients.[6] Impaired recruitment and migration of cells to wound sites also decreases the production of chemokines essential for wound repair.[2,6,7] Therefore, one of the main strategies for treating diabetic wounds should be to improve angiogenesis.[9,10] Although several studies have demonstrated that growth factor treatments improve angiogenesis, short half-lives and adverse effects limit the success of these treatments.[6,7,9]

Recombinant human bone morphogenetic protein-2 (rhBMP2) has been approved by the FDA and is used clinically for bone regeneration.[11] In addition, several studies have demonstrated the crucial role of BMP2 in physiological development and vascular homeostasis[12] including angiogenesis.[13-15] BMP signaling regulates various processes including mesoderm formation, vasculogenesis, sprouting angiogenesis, arteriovenous differentiation, endothelial barrier function, and endothelial-to-mesenchymal transition.[12,16] Furthermore, BMP signaling affects endothelial cell (EC) migration, proliferation, and network formation.[12] During sprouting angiogenesis, BMP signaling promotes vascular morphogenesis by regulating vascular activation and maturation.[12] BMP2 also induces *in vitro* proliferation of the human pulmonary artery and aortic ECs, increases migratory efficiency, and promotes tube formation of human dermal microvascular ECs, and human aortic and umbilical vein ECs.[12,14,17-20]

The angiogenic ability of BMP2 led us to hypothesize whether it could improve diabetic wound healing. However, little research has been conducted on the association of BMP2 with wound healing. Because BMP2 can affect bone

formation, side effects could include ectopic ossification or vascular calcification.[21,22] However, another recent study has reported that activation of BMP signaling is involved in stem cell recruitment to wound sites and in wound healing acceleration.[23]

The short half-life of rhBMP2 requires that it be administered at a high dosage to be effective. Research to overcome this limitation have been actively conducted. In a previous study, using the protein transduction domain (PTD), a recombinant PTD-fusion polypeptide was delivered intracellularly across the membrane without any specific receptor.[24,25] After transduction, the PTD-fusion polypeptide refolded, cleaved post-translationally, and was secreted in its active form.[11,25,26] We reported PTD-BMP2 as a prodrug of BMP2 using this strategy.[11] It showed improved functionality *in vivo* with a lower dose than rhBMP2.[11] Furthermore, to overcome the size limitation imposed by endosomal cellular delivery, we previously developed a PTD-BMP-7 formulated in micelle as lipid nanoparticle (LNP).[27] The micelle improved endosomal transduction of PTD-BMP-7, and micellized PTD-BMP-7 was successfully processed and secreted as active BMP-7.[27]

We hypothesize that the newly designed PTD-BMP2 formulated in micelle could transduce the wound and secrete successfully active BMP2 and that angiogenesis could be enhanced by BMP2, and it could improve the cell recruitment and reparative process of wound healing.

This study aimed at investigating whether LNP formulated PTD-BMP2 (LNP-PTD-BMP2) can successfully transduce a diabetic wound when applied via a gelatin hydrogel dressing and whether the angiogenic function of BMP2 can

improve diabetic wound healing.

II. MATERIALS AND METHODS

1. Preparation of LNP-PTD-BMP2

Recombinant PTD-BMP2 was synthesized as described previously.[11] The PTD-fusion BMP2 polypeptide was amplified using pRSET (Invitrogen), a bacterial expression vector that contains an Xpress epitope and a His tag. The precursor cDNA of BMP2 was PCR-amplified from the cDNA of Saos-2 osteosarcoma cells. The TAT sequences (RKKRRQRRR) for the PTD domain were inserted next to the epitope, and the precursor cDNAs of BMP2 were cloned into a TAT-expression cassette. After the transformation of BL21 competent cells and IPTG induction, inclusion bodies were obtained from the insoluble fraction using 1% Triton X-100 buffer. The insoluble fraction was solubilized with an 8 M urea solution, and the recombinant protein was purified using Ni-Ti beads and imidazole elution. Buffer shock was then used to imbue high surface energy (ΔG) properties. Denatured polypeptides were micellized with filtered 0.1% egg lecithin (BOC Sciences, Shirley, NY, USA) via bath sonication.[27]

2. Preparation of LNP-PTD-BMP2-loaded gelatin hydrogel

Gelatin hydrogel (GH) was synthesized as previously described.[28,29] Gelatin gels were prepared by cross-linking gelatin via microbial transglutaminase (mTG). TI transglutaminase formula (Modernist Pantry) was dissolved in phosphate-buffered saline (PBS) to obtain a 10% (wt, weight ratio) solution, followed by addition of gelatin (Sigma-Aldrich) at 5.5% (w/v%:

weight/total solution volume) in PBS. GHs were prepared by mixing the appropriate volume of the 10% mTG solution with 5.5% (w/v%) gelatin, according to the experimental need. As previously described, 4.4% gelatin hydrogel at 200 μl/cm^2 was used.[29] The GH, mTG solution, and LNP-PTD-BMP2 were mixed together at room temperature.

3. In vitro wound healing study (enhanced cell recruitment study)

In vitro wound healing was assessed using a scratch wound assay as previously described.[30,31] HaCaT cells were seeded at densities of 2×10^5 cells/ml into 6-well plates and incubated at 37 °C under 5% CO_2. When the cells reached a confluence of 80–90%, they were scratched with 200-μl micropipette tips. Floating cells were immediately removed by washing them away with PBS, and 1.5 ml of the culture medium was added. rhBMP2 and LNP-PTD-BMP2 were added at concentrations of 100 ng/ml each. After up to 48 h of cell culture, a digital camera (Nikon, Tokyo, Japan) coupled to an optical microscope (Nikon TMS) was used to capture the images. Quantification of the percentage of wound closure between 0 h and 48 h were assessed using ImageJ (Ver. 1.48, Aspire Software International, Leesburg, VA, USA). All experiments were repeated at least three times.

4. HaCaT cell proliferation assay with LNP-PTD-BMP2

The proliferation of HaCaT cells by LNP-PTD-BMP2 was evaluated using a water-soluble tetrazolium salt (WST) assay (EZ-Cytox Kit, Daeil Lab Service, Seoul, Korea). First, HaCaT cells were seeded in 12-well plates at a

density of 1×10^4 cells/ml and incubated with 100 ng/mL LNP-PTD-BMP2 for 24, 72 and 120 h at 37 °C, 5% CO_2. Then, 10 μl of EZ-Cytox solution was added to each well and the cells were incubated at 37 °C for 3 h. The absorbance was measured at 450 nm. All samples were tested in triplicate.

5. In vitro angiogenesis study via tube formation assay

The EC migration and capillary tube formation assays are used to assess angiogenesis *in vitro*.[32,33] The human umbilical vein endothelial cell (HUVEC) capillary tube formation assays were performed to assess LNP-PTD-BMP2 induced angiogenesis *in vitro*.[33]

Primary HUVECs (Lonza, Basel, Switzerland) were cultured in endothelial cell growth medium-2 (EBM-2, Lonza) supplemented with 10% fetal bovine serum (FBS, Gibco-Invitrogen), 100 units/ml penicillin G, and 100 μg/ml streptomycin at 37 °C under 5% CO_2/95% air. All cells used in experiments underwent fewer than eight passages after resuscitation.[33] Further, 500 ng of LNP-PTD-BMP2 was added to the HUVEC culture medium, and the medium was allowed to sit overnight. The insoluble fractions of cells were used for western blotting to detect transduced recombinant protein in cells.

The tube-like structures formed by HUVECs on Matrigel with reduced quantities of growth factors were analyzed as previously described.[34-36] Ninety-six-well culture plates were coated with Matrigel (50 μl/well) and incubated for 30 min at 37 °C. After HUVECs were cultured in EBM-2 containing 1% FBS, they were plated onto the layer of Matrigel at a density of 2×10^4 cells/well. Following incubation at 37 °C for 2 h, the cells were treated with either H_2O_2 (200

nM), rhBMP2 (100 ng) with H_2O_2 (200 nM), or LNP-PTD-BMP2 (100 ng) with H_2O_2 (200 nM). Each well was analyzed at 1 h intervals for up to 6 h. Tube formation was observed using an inverted phase contrast microscope, and the number of nodes and tubes were quantified.

6. BMP2 release test and diabetic wound healing study in vivo

A. Preparation of streptozotocin (STZ)-induced diabetic mouse model

ICR mice (male, 7 weeks old) were purchased from Orient Bio (Seoul, Korea). All the mice were housed in wire cages. The temperature and humidity of cages were controlled at 20–22 °C and 40–50%, respectively, throughout the experiment. All mice were induced Type I diabetes by STZ (Sigma-Aldrich) injection intraperitoneally at dose of 200 mg/kg body weight dissolved in 0.05 M citrate buffer, pH 4.5. After one week, a diabetic phenotype was confirmed with blood glucose level exceeded 300 mg/dl by a OneTouch Select meter (Johnson & Johnson, UK). The animal studies were carried out in accordance with guidelines set by the Department of Laboratory Animal Resources (Permit No. 2018-0325) at the Yonsei University College of Medicine, Seoul, South Korea.

B. Diabetic wound treatment with rhBMP2 or LNP-PTD-BMP2-loaded gelatin hydrogel dressings

Mice (male, 9 weeks old) were anesthetized by intraperitoneally injecting Zoletile (30 mg/kg body weight) and Rumpon (10 mg/kg body weight). The hair on the backs of the mice were shaved and wiped with 70% ethanol. Full-thickness skin wounds (10 mm in diameter) were created on the backs of diabetic mice.

Silicone rings were sutured around each wound to prevent wound contraction.[37,38]

The wounds were filled with control GH, rhBMP2-loaded GH, or LNP-PTD-BMP2-loaded GH (5 mice/group) using a pipette (Fig. 1). After applying the experimental materials, all wounds were covered with Vaseline gauze (Covidien, USA), which was used as a moist dressing to minimize GH dehydration. The concentration of rhBMP2 was 100 ng/cm^2. After concentration optimization, the concentrations selected for LNP-PTD-BMP2 were 0, 25, 100, and 400 ng/cm^2. The wound sites were treated with the control GHs, rhBMP2-loaded GHs, and LNP-PTD-BMP2-loaded GHs once after surgery, and the wound dressing and gauze were changed twice a week.

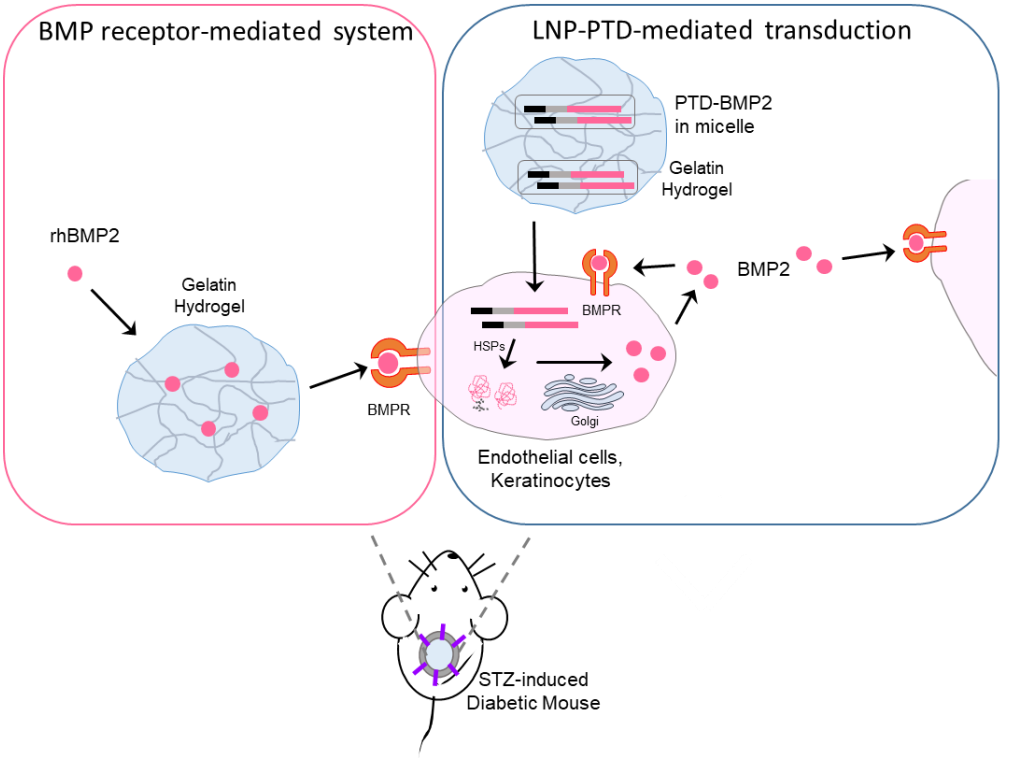

Figure 1. Schematic illustration of the approaches used. The back wound of a STZ-induced diabetic mouse treated with rhBMP2 or LNP-PTD-BMP2-loaded gelatin hydrogel. After intracellular transduction of micellized PTD-BMP2 and processing occurred, active BMP2 was secreted and was followed by autocrine and paracrine action.

C. Measurement of BMP2 release

ICG-labeled rhBMP2- or LNP-PTD-BMP2-loaded GH was applied on the wound site. After dressing the wound, *in vivo* near-infrared fluorescent images were captured at 0, 1, 3, 5, and 7 days using an animal optical imaging system (IVIS, Caliper Life Sciences, MA, USA). During imaging, mice were kept under the inhaled anesthesia isoflurane. The excitation and emission wavelengths of ICG were 780 and 831 nm, respectively. The fluorescence signal ($p/s/cm^2$) from each mouse was measured using Living Image (version 2.50, Xenogen). All tests were carried out in 5 mice.

D. Measurement of wound closure

Photographs of the wounds were taken using a digital camera (Nikon, Japan) at days 0, 3, 7, 10, and 14. To evaluate the degree of wound closure, the wound area was measured using ImageJ. The wound area on the indicated day (A_t) relative to the initial wound area (A_0) (%) was calculated as $(A_0 - A_t)/A_0 \times 100$.

E. Histological analysis of regenerative tissues

At the time of sacrifice, perilesional skin samples were collected and fixed in 10% formalin solution. The skin samples were stained with hematoxylin and eosin (H&E) and Masson's trichrome (MT). The wound area was analyzed digitally using ImageJ. The distance between the regenerated keratinocyte cell layers was measured on both ends of the wound. The re-epithelialization rate was determined by comparing the measured distances with those in the initial wound

images of MT-stained histological sections.

Collagen deposition of regenerated skin tissue at 14 days was measured by counting the pixels in MT-positive blue areas of granulation and assessing the staining intensity, using ImageJ for quantitative analysis. Von Kossa staining was used to evaluate calcium deposition on regenerated perilesional skin tissue. A total of five mice per group was analyzed to determine the histology of the regenerated tissues.

F. Immunofluorescence

The sections were collected from the central wound area for immunofluorescence analysis. They were deparaffinized and rehydrated. After washing the sections twice with PBS, they were incubated with H_2O_2 for 10 min to suppress endogenous peroxidase activity in order to reduce nonspecific background staining. The sections were washed twice again with PBS and then incubated overnight at 4 °C with primary antibodies against CD31 (50:1, Abcam Inc., MA, USA) to detect EC and against α-SMA (α-smooth muscle actin, Sigma-Aldrich) to detect vascular smooth muscle cells formed during neovascularization. Subsequently, the sections were washed three times with PBS. Phycoerythrin-conjugated goat anti-rabbit secondary antibodies (Santa Cruz Biotechnology Inc., CA, USA) were added for visualization of the primary antibodies. For nuclei staining, 4′,6-diamidino-2-phenylindole (Sigma-Aldrich) was used. The images were taken using an inverted fluorescence microscope (IX-71, Olympus, Tokyo, Japan). To determine whether the angiogenic ability of diabetic mouse model decreased, the wound sections were compared between ICR mice and diabetic

mice.

7. Statistical analysis

All data were given as the mean ± standard deviation. Statistical analysis was performed using SPSS 25.0 software (SPSS Inc., Chicago, USA). One-way analysis of variance (ANOVA) and post hoc analysis were used to identify the differences between groups. * indicates $p < 0.05$, ** indicates $p < 0.01$, and *** indicates $p < 0.001$.

III. RESULTS

1. Concentration optimization of LNP-PTD-BMP2

To determine the optimal concentration of LNP-PTD-BMP2, we loaded LNP-PTD-BMP2 in GHs at concentrations of 0, 0.4, or 4 μg/cm^2 (Fig. 2). We found that a concentration of 0.4 μg/cm^2 showed a significantly enhanced wound closure capacity, while a concentration of 4 μg/cm^2 revealed no significant wound closure effect when compared to the defect group (Fig. 2A, 2B). Moreover, similar results were found in the neovascularization study (Fig. 2C). Therefore, we subdivided the concentrations to 0, 25, 100, and 400 ng/cm^2 and obtained the wound healing capacity and neovascularization results (Fig. 3). LNP-PTD-BMP2 concentrations of 100 ng/cm^2 and 400 ng/cm^2 showed a significantly enhanced wound closure capacity and collagen deposition when compared to those in the defect group, control group, and groups with lower concentrations (Fig. 3A, 3B, 3E, 3F). As a result of comparing the neovascularization capacity of different concentrations in an immunofluorescence study, 100 ng/cm^2 and 400 ng/cm^2 of

LNP-PTD-BMP2 revealed a significantly greater number of CD31-positive cells than the defect group, control group, and groups with lower concentrations did (Fig. 3C, 3D). Although 400 ng/cm^2 of LNP-PTD-BMP2 revealed a significantly greater rate of CD31-positive cells compared to that at 100 ng/cm^2 concentration, it also showed mild wound inflammation. Finally, we selected 100 ng/cm^2 as the optimal LNP-PTD-BMP2 concentration.

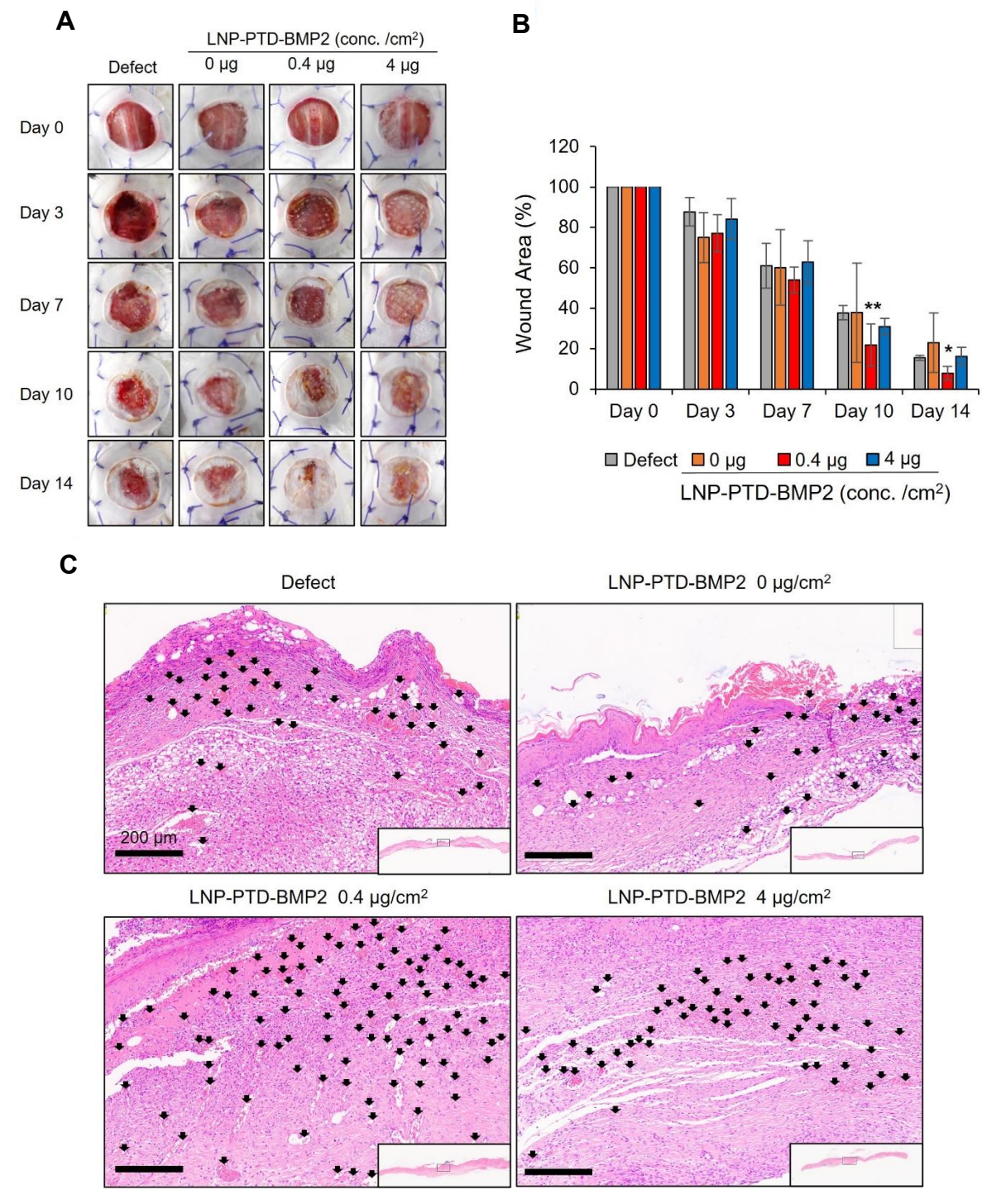

Figure 2. Concentration optimization of LNP-PTD-BMP2(1). (A) Large full-thickness back skin wounds were inflicted on STZ-induced diabetic mice and filled with LNP-PTD-BMP2-loaded GH at concentrations of 0, 0.4, and 4 μg/cm^2. The photographs of the wounds were taken on days 0, 3, 7, 10, and 14. (B) Quantitative analysis of wound closure rate for each concentration. (C) H&E-stained microscopic images of newly formed red capillary vasculature (black arrows) in the regenerated tissue for each concentration on day 14.

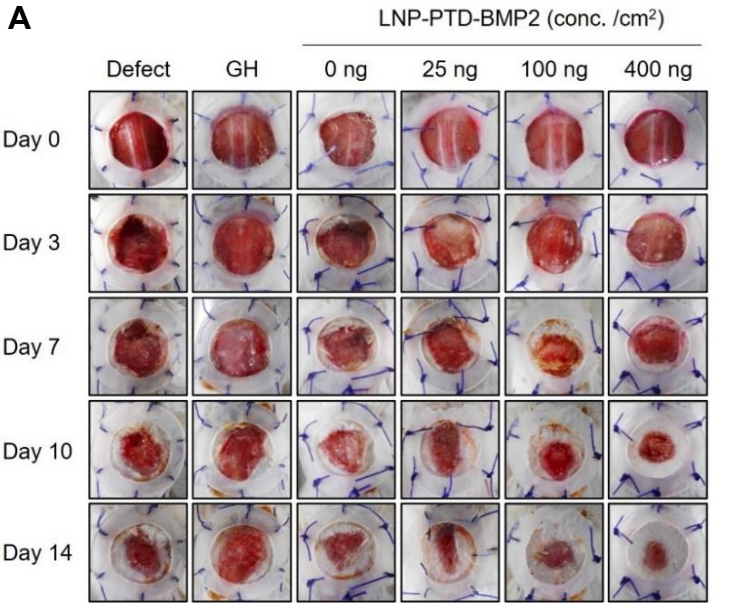

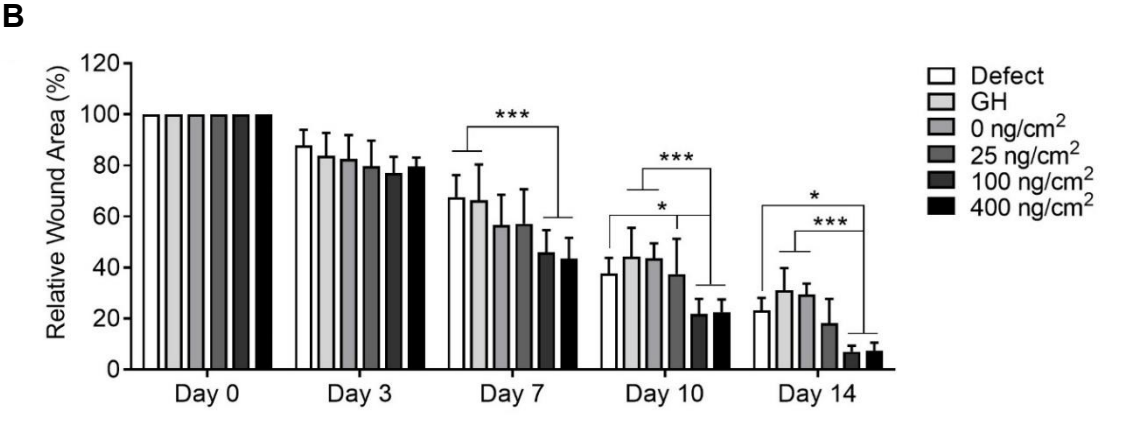

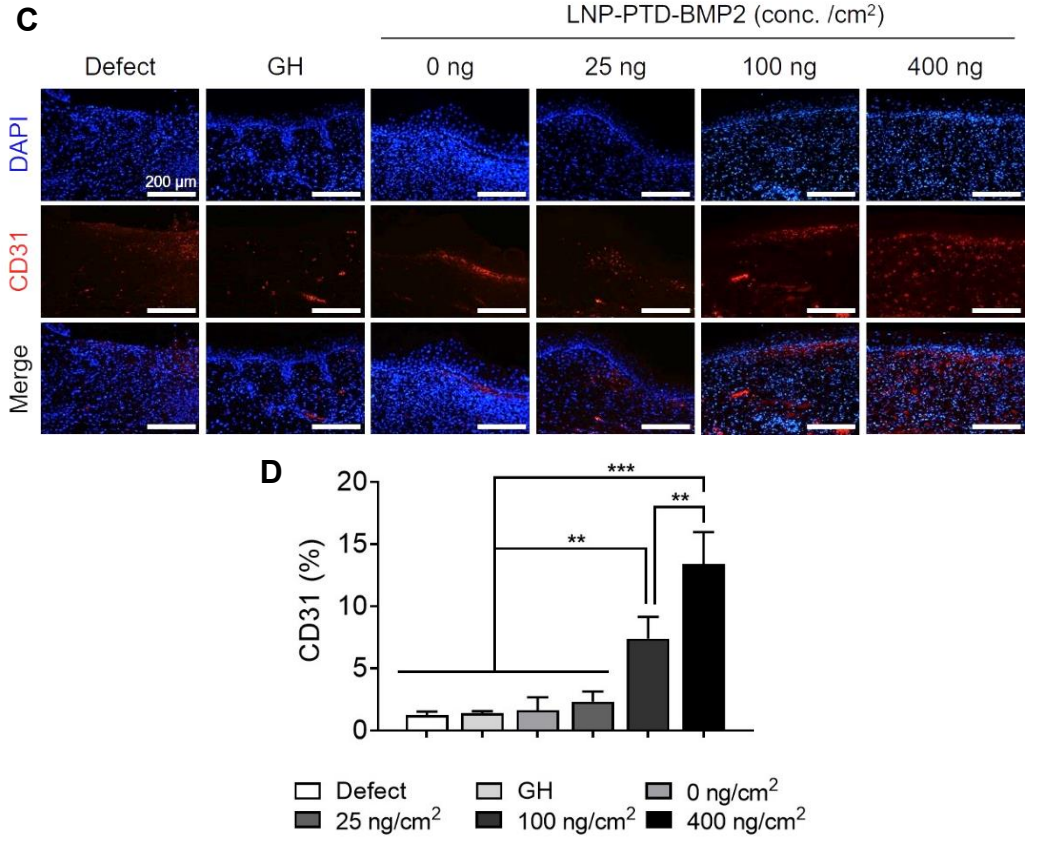

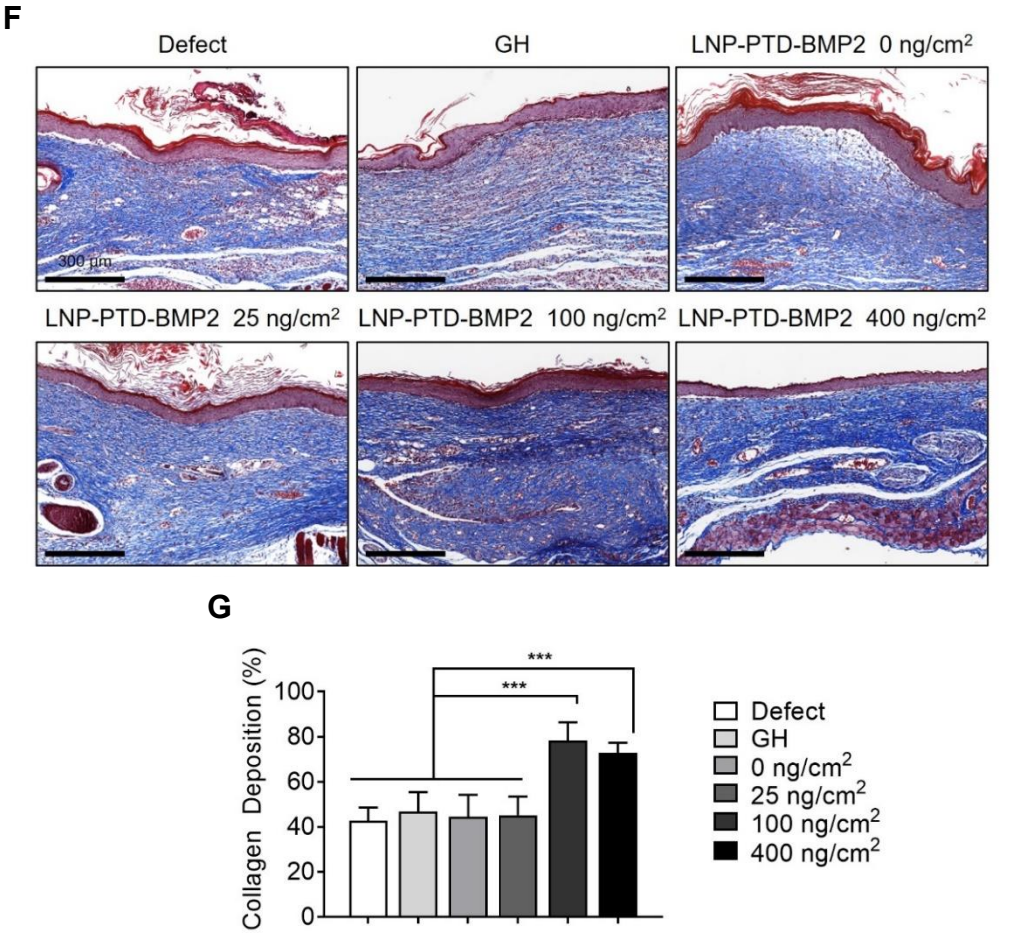

Figure 3. Concentration optimization of LNP-PTD-BMP2(2). (A) Large full-thickness back skin wounds created in STZ-induced diabetic mice were filled with GH and LNP-PTD-BMP2-loaded GH at concentrations of 0, 25, 100, and 400 ng/cm^2. Representative images show the skin wounds on days 0, 3, 7, 10, and 14. (B) Quantitative analysis of wound healing rate relative to the initial wound over time. (C) Immunofluorescence staining shows expression of CD31 in regenerated wound tissues on day 14. (D) Quantitative analysis of CD31-positive cells. (E) H&E-stained microscopic images of newly formed red capillary

vasculature (black arrows) in the regenerated tissue for each concentration of 0, 25, 100, and 400 ng/cm^2 on day 14. (F) MT-stained regenerated soft tissues imaged on day 14. The granulation tissue showed the deposition of newly formed collagen tissues (blue areas). (G) Quantitative analysis of collagen deposition for each concentration. All quantitative analyses were performed using ImageJ.

2. Wound healing, cell proliferation, and angiogenesis study of LNP-PTD-BMP2 in vitro

A scratch wound healing assay on HaCaT cells was conducted to evaluate the efficacy of LNP-PTD-BMP2 in inducing *in vitro* wound healing in comparison with that of rhBMP2 (Fig. 4A). The HaCaT cells treated with LNP-PTD-BMP2 showed a significantly enhanced cell recruitment capacity when compared to that of the control and rhBMP2 treatments and showed 81.3% wound gap closure at 48 h (Fig. 4B).

To determine the effect of LNP-PTD-BMP2 on the proliferation capacity of HaCaT cells, the WST assay was performed (Fig. 4C). The proliferative capacity of HaCaT cells treated with LNP-PTD-BMP2 showed no significant differences compared to that in the control group. This result suggests that LNP-PTD-BMP2 does not inhibit the growth of HaCaT cells.

HUVEC capillary tube formation assays were performed to assess LNP-PTD-BMP2-induced angiogenesis *in vitro* (Fig. 4D). To mimic the *in vitro* diabetic environment, we added H_2O_2 to the cells. Images were obtained after 6 h and quantified. Compared to the control and rhBMP2 treatments, the LNP-PTD-BMP2 treatment showed significantly higher tubes and node formation

capacity (Fig. 4E). Intracellular transduction efficiency of LNP-PTD-BMP2 was confirmed by western blot analysis. (Fig. 4F).

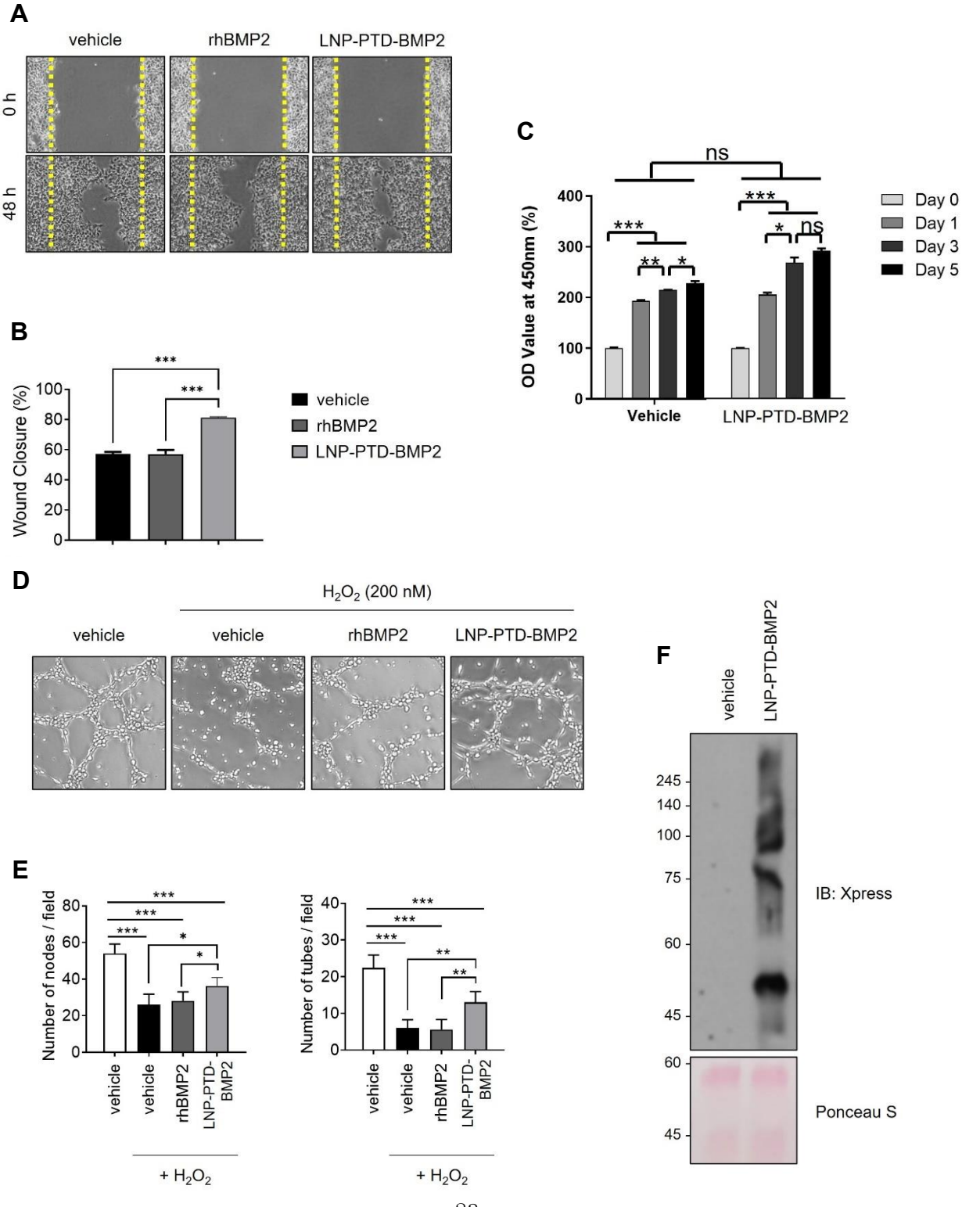

Figure 4. LNP-PTD-BMP2 increased migration and angiogenesis *in vitro.* (A) Incubated HaCaT cells (2×10^5 cells/ml) were scratched and treated with rhBMP2 (100 ng/ml) or LNP-PTD-BMP2 (100 ng/ml). After being cultured for 48 h, the gap differences were measured from time zero. (B) Wound closure rates were quantified using ImageJ. (C) WST assay was performed to determine the proliferative capacity of LNP-PTD-BMP2-treated HaCaT cells. Each experiment was performed in triplicate (n = 3). All the error bars indicate ± SEM. (D) HUVECs were treated with vehicle, H_2O_2 presenting with vehicle, H_2O_2 presenting with rhBMP2 (100 ng), or H_2O_2 presenting with LNP-PTD-BMP2 (100 ng) for tube formation assays. Representative images were taken after 6 h. (E) Number of nodes and tubes were quantified. Results of five independent experiments are presented. (F) HUVECs were treated with 500 ng of LNP-PTD-BMP2 overnight, and the insoluble fraction was used for western blotting.

3. In vivo BMP2 release profile of LNP-PTD-BMP2-loaded GH

ICG labeling was used to investigate the *in vivo* BMP2 release profile of the rhBMP2- or LNP-PTD-BMP2-loaded GH. *In vivo* near-infrared fluorescent images were acquired using an animal optical imaging system (Fig. 5A). Wounds treated with LNP-PTD-BMP2-loaded GH exhibited high fluorescent intensity until day 7 (Fig. 5B). The fluorescent intensity of wounds treated with rhBMP2-loaded GH significantly diminished beginning on day 5. Therefore, LNP-PTD-BMP2 showed more stably sustained release and a longer half-life than rhBMP2.

A

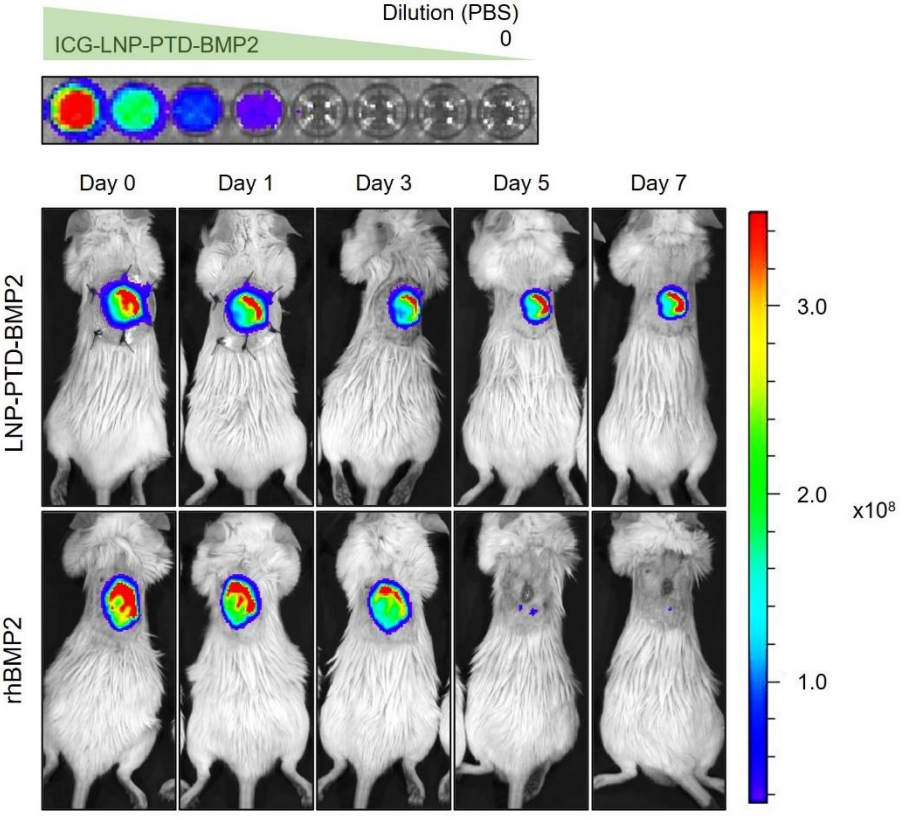

B

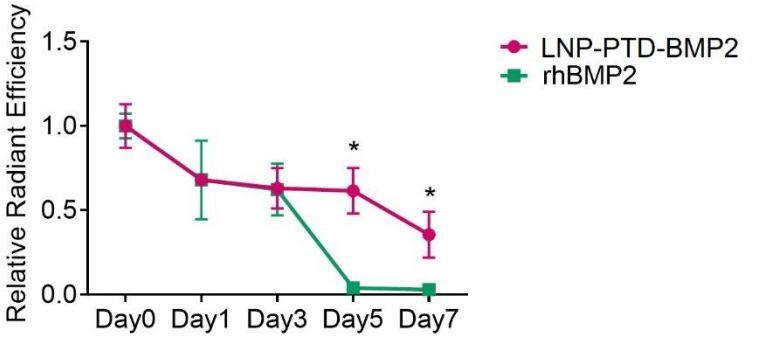

Figure 5. *In vivo* BMP2 release profile of rhBMP2- or LNP-PTD-BMP2-loaded GH using ICG labeling. (A) ICG signal from the back wounds was observed using IVIS at 1, 3, 5, and 7 days after treatment of STZ-induced diabetic mice with ICG-labeled rhBMP2- or LNP-PTD-BMP2-loaded GH. Wounds treated with LNP-PTD-BMP2-loaded GH remained exhibited high fluorescence intensity until day 7, while wounds treated with rhBMP2-loaded GH abruptly diminished beginning on day 5. (B) Relationship of the relative radiant efficiency of ICG-labeled LNP-PTD-BMP2 and rhBMP2 showed that LNP-PTD-BMP2 is more stable and exhibits longer-term release than rhBMP2.

4. Wound closure and histological changes of LNP-PTD-BMP2 in diabetic wound healing

We confirmed decreased wound healing capacity in an STZ-induced diabetic mouse model, as observed in human diabetic patients (Fig. 6A, 6B).[39] Further, we investigated the effect of rhBMP2 or LNP-PTD-BMP2-loaded GH on wound closure in this model (Fig. 6C, 6D). Wounds treated with LNP-PTD-BMP2-loaded GH showed a significantly enhanced regeneration capacity when compared to that of the control wounds after day 3. When compared to wounds treated with rhBMP2-loaded GH, wounds treated with LNP-PTD-BMP2-loaded GH showed significantly decreased wound size after day 7. There was no significant difference over time in wound healing between rhBMP2-loaded GH and control wounds.

To investigate re-epithelialization rate and collagen deposition, we analyzed the regenerated skin tissues using H&E and MT staining on day 14. The

epithelial layer of wound sites treated with LNP-PTD-BMP2-loaded GH showed the best re-epithelialization rate among the wounds for control and treated with rhBMP2-loaded GH (Fig. 6E, 6F). The rhBMP2-loaded GH dressing showed a similar re-epithelialization rate to the control ($p = 0.779$). Wounds treated with LNP-PTD-BMP2-loaded GH showed significantly higher collagen deposition than control defect wound (3.3-fold) and wounds treated with rhBMP2-loaded GH (4.1-fold) (Fig. 6G, 6H).

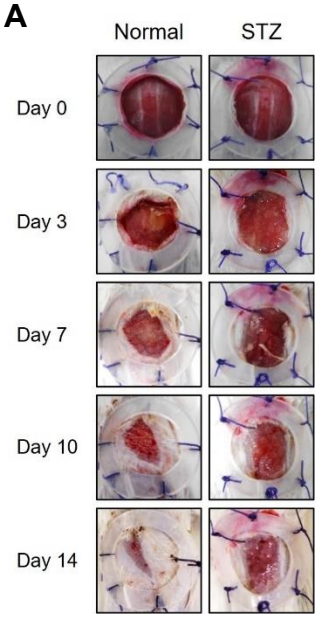

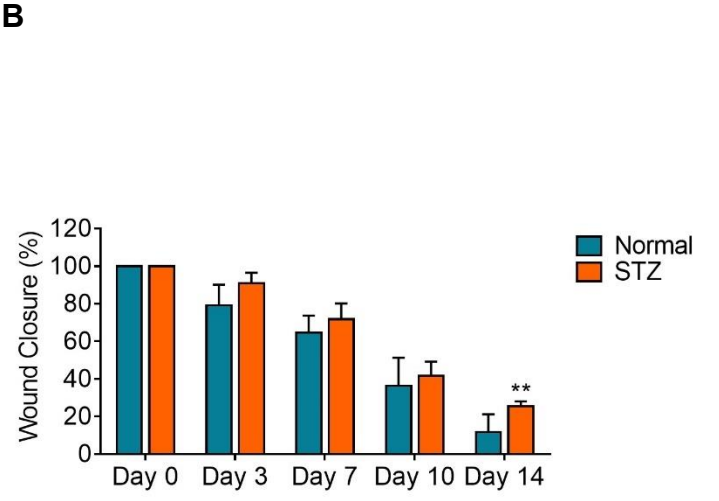

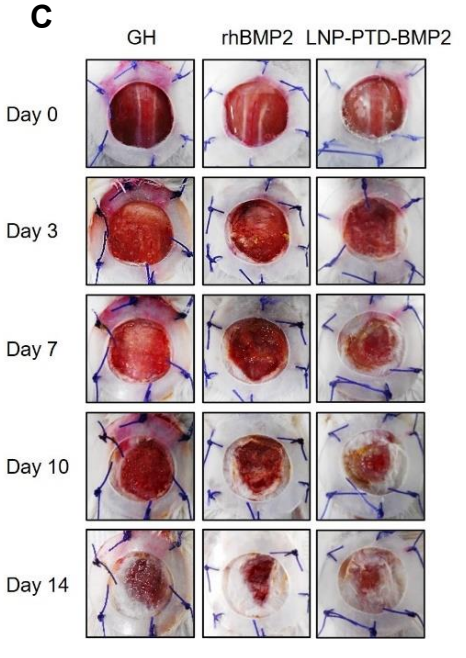

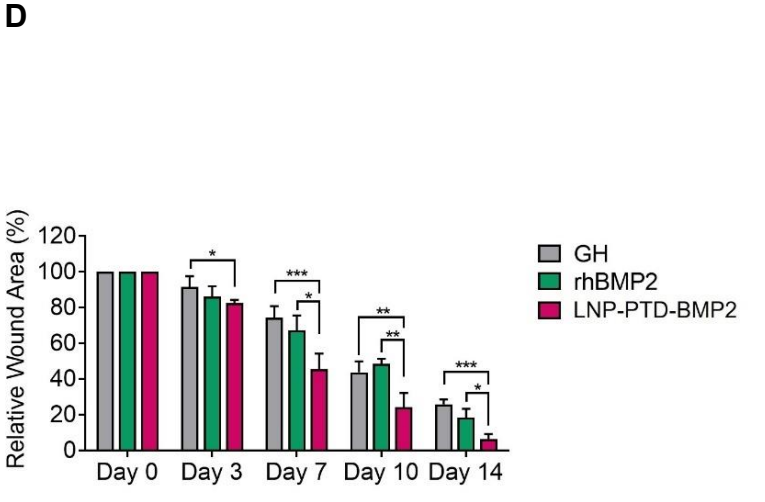

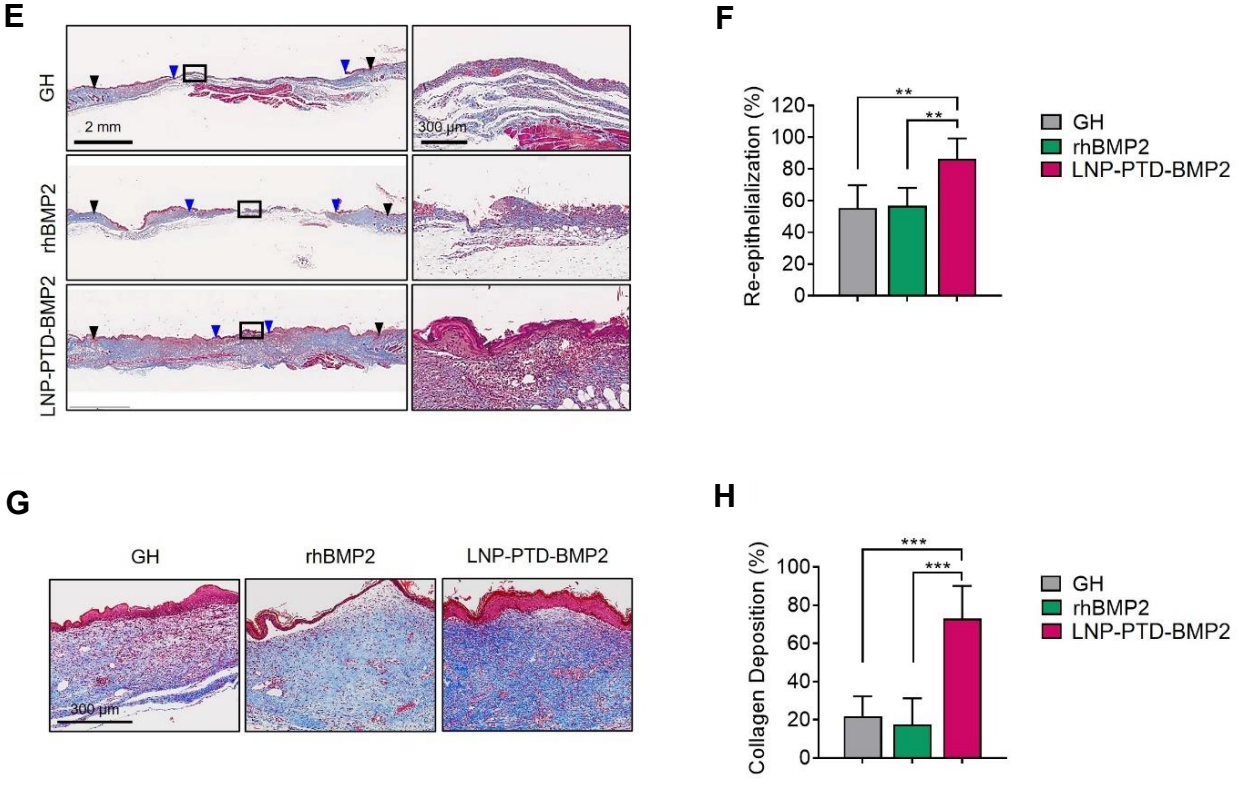

Figure 6. Comparisons of wound closures and histological changes between rhBMP2- and LNP-PTD-BMP2-loaded GHs in diabetic wound healing. (A) Comparison of wound healing capacity between a healthy and an STZ-induced diabetic mouse. Full-thickness back skin wounds of both mice were photographed on days 0, 3, 7, 10, and 14. (B) Quantitative analysis of wound closure rate relative to the initial wound size over time between healthy and STZ-induced diabetic mouse. (C) Wound healing effects of rhBMP2- and LNP-PTD-BMP2-loaded GH in the STZ-induced diabetic mice. rhBMP2 (100 ng/cm^2)- and LNP-PTD-BMP2 (100 ng/cm^2)-loaded GHs were applied to the back wounds. Photographs of wounds were obtained on days 0, 3, 7, 10, and 14. (D)

Quantitative analysis of wound healing rate relative to the initial wound over time. (E) MT-stained microscopic images were obtained on day 14 to assess the re-epithelialization rate. Black boxes indicate the portion of the remaining wounds. Black arrowheads indicate the ends of the initial wound. Blue arrowheads indicate the ends of the regenerated keratinocyte cell layer. (F) Quantitative analysis of re-epithelialization rate. (G) Regenerated soft tissues were stained with MT, and microscopic images were obtained on day 14. MT-positive blue areas of granulation tissue indicate deposition of newly formed collagen tissues. (H) Quantitative analysis of collagen deposition using ImageJ.

To evaluate whether BMP2 causes calcification of wounds and regenerated tissue, we analyzed regenerated skin perilesional tissues with Von Kossa staining on day 14. No calcium depositions were observed in diabetic mice treated with the control, rhBMP2-loaded GH, or LNP-PTD-BMP2-loaded GH (Fig. 7).

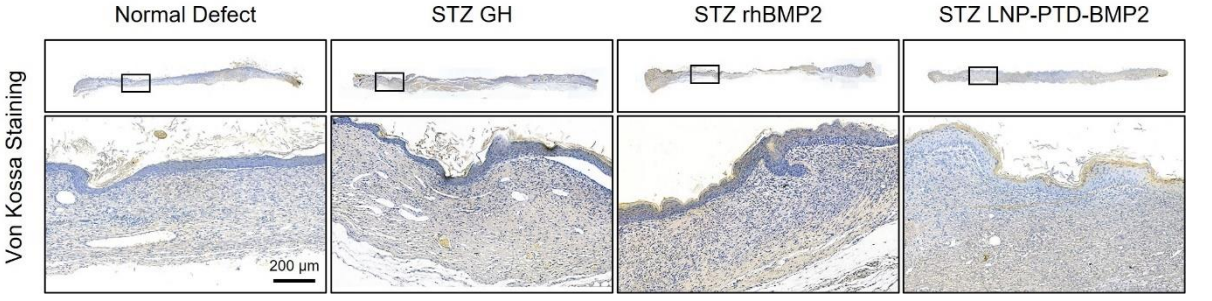

Figure 7. Histological evaluation of calcific deposition in regenerated tissue treated with rhBMP2- or LNP-PTD-BMP2-loaded GH. Von Kossa staining of regenerated skin perilesional tissues showed no calcific deposit on day 14.

5. Neovascularization of LNP-PTD-BMP2 in diabetic wound healing

To assess wound neovascularization, we used H&E staining, CD31, and α-SMA immunofluorescence labeling. The number of red capillary vasculatures with the H&E staining were significantly greater in wounds treated with LNP-PTD-BMP2-loaded GH than in control wounds or in wounds treated with rhBMP2-loaded GH (Fig. 8A, 8B). The numbers of CD31-positive cells and α-SMA positive-cells were significantly greater in wounds treated with LNP-PTD-BMP2-loaded GH than control wounds or wounds treated with rhBMP2-loaded GH (Fig. 8C, 8D). The rate of CD31-positive cells in wounds treated with LNP-PTD-BMP2-loaded GH was 1.7- and 1.8-fold higher than the rates of control wounds and wounds treated with rhBMP2-loaded GH, respectively. The rate of α-SMA-positive cells was also found to be 2.9- and 3.1-fold higher, respectively.

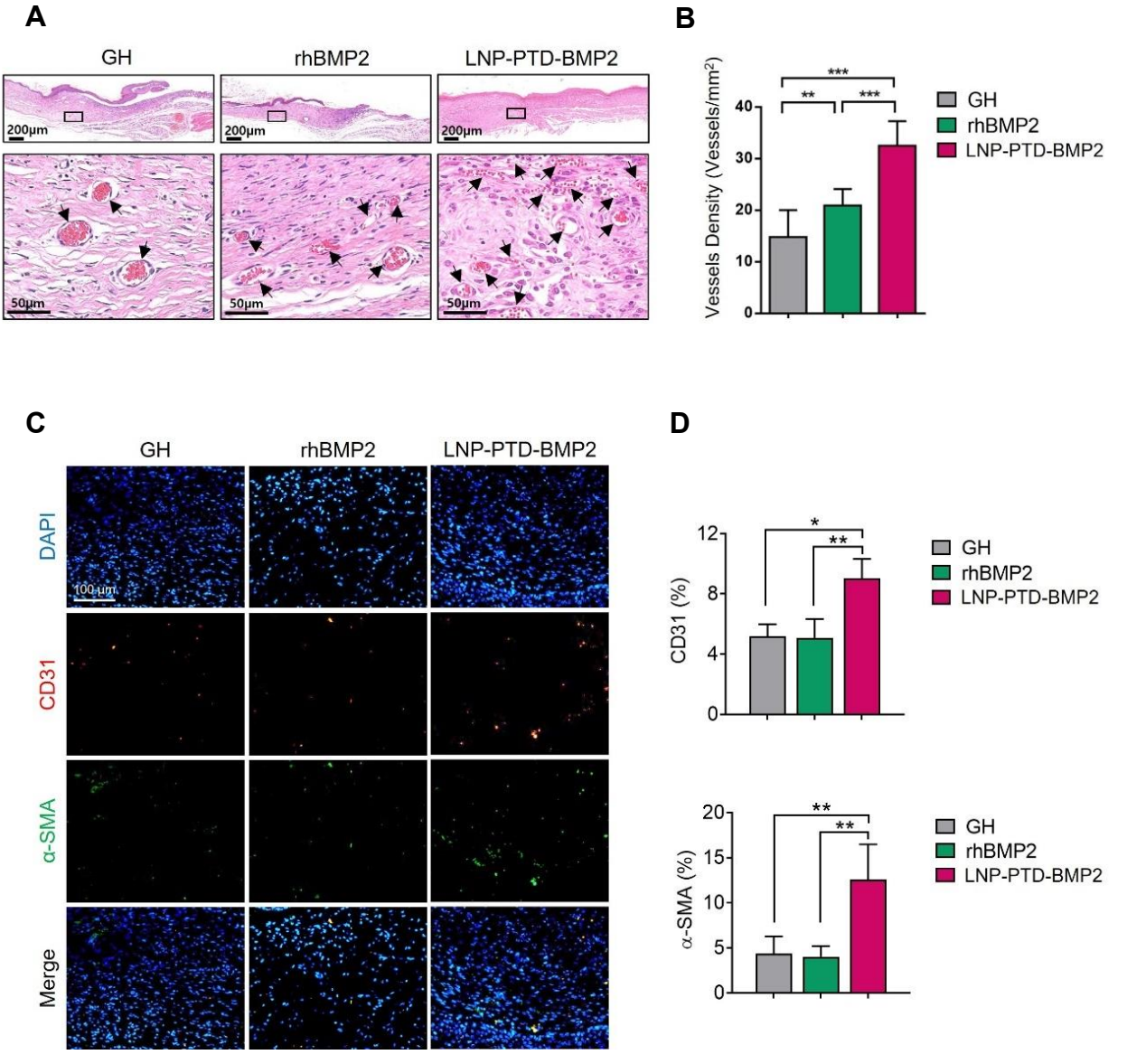

Figure 8. Neovascularization effects of rhBMP2- and LNP-PTD-BMP2-loaded GH in STZ-induced diabetic mice on day 14. (A) Microscopic images of newly formed red capillary vasculature (black arrows) in the regenerated tissue obtained using the H&E staining. (B) The newly formed red capillary vasculatures were

enumerated. (C) Immunofluorescence study shows CD31-positive cells (red) and α-SMA-positive cells (green) in the regenerative tissue, suggesting the generation of mature vessels. (D) Quantitative analysis of CD31- and α-SMA-positive cells using ImageJ.

IV. DISCUSSION

The capacity for angiogenesis is decreased in diabetic chronic wounds and plays a critical role in the pathogenesis of wound healing impairment.[6,7] Various studies have been performed to identify treatments that improve angiogenesis in chronic wounds. Previous therapeutic approaches have used growth factors, endothelial progenitor cells, and stem cells, but the results have been limited.[40-43]

As a member of the TGF-beta superfamily, BMP was first known to be capable of inducing bone formation. rhBMP2 has been widely used for spinal fusion in orthopaedic surgery. It has shown promising results, but complications were reported in studies using high doses, with 9.9% of patients with anterior cervical fusion who used a high dose developing a hematoma after surgery.[44-46] Among them, 73.3% developed a hematoma 4–5 days after surgery.[44] The hematomas that were correlated with a high dose of rhBMP2 showed a higher frequency and later onset than other hematomas that occurred in patients who undergo anterior cervical fusion without rhBMP2.[44] This report led to the idea that BMP2 may also be involved in angiogenesis.

BMP2 has been gradually revealed to play an essential role in pathobiological processes and the homeostasis of skin and various tissues.[47] As described previously in this article, BMP2 induces chemotaxis in microvascular ECs.[40,48] In 70% of patients with familial pulmonary arterial hypertension, which is an uncommon vascular disorder, BMP2 receptor mutations were identified.[49-51] Decreased expression of BMP2 receptors in lung tissues leads to EC dysfunction, resulting in increased vascular resistance.[12,49,52,53] In fetal skin,

BMP2 promotes dermal and epidermal growth and seems to be involved in wound healing.[54] Treatment with BMP2 could thus be an ideal therapy for diabetic wound healing. This study supports the angiogenic and wound healing capacity of BMP2 *in vitro* and *in vivo*.

However, rhBMP2 is difficult to use for healing wounds due to limitations such as short half-life.[11,55] To overcome this limitation, we used a novel delivery method utilizing PTD formulated in micelle. In a previous study, micellized PTD-BMP-7 was transduced directly into cells via an endosomal pathway, and active BMP-7 was successfully secreted in HEK 293 cells.[27] In our study, LNP-PTD-BMP2 was successfully transduced into cells independent of the BMP2 receptor to secrete active BMP2 (Fig. 4F). In another study, PTD-BMP-7 injected intraperitoneally in Balb/C nude mice showed five times longer half-life and nine times more area under the curve than rBMP-7 in intravital fluorescence imaging.[25] We found also that LNP-PTD-BMP2 has a longer half-life and duration of effect compared to rhBMP2 (Fig. 5). Furthermore, when LNP-PTD-BMP2 was loaded into a GH and used topically, it was observed locally around the wound without a systemic effect, as shown in the *in vivo* BMP2 release study (Fig. 5).

Previous studies found that BMP2 promotes vascular calcification, which is similar to osteoblast differentiation in vessels.[22] However, in this study, we confirmed the absence of calcific deposits around the regenerative tissue via Von Kossa staining (Fig. 7). Furthermore, based on the BMP2 release profile from the GH, the effect was observed locally around the wound without any systemic effect (Fig. 5A). Meanwhile, Lewis et al. demonstrated that BMP signaling

inhibits keratinocyte proliferation and migration in skin epithelium during wound healing.[56] In another study, BMP2 and BMP-4 negatively affect keratinocyte proliferation.[56-58] It is thought that different experimental settings or the half-life of BMP2 constructs may influence the results. In our study, we found that LNP-PTD-BMP2 enhanced keratinocyte migration and did not inhibit proliferation *in vitro* (Fig. 4A, 4B, 4C). Furthermore, in our experimental settings with LNP-PTD-BMP2, we observed both the *in vitro* and *in vivo* results of fibroblasts, ECs, and keratinocytes in the wound healing process of normal and diabetic mice. In this study, we used BMP2 as an active form after transduction, and angiogenesis and migration were improved through a more prolonged effect, which is thought to affect wound healing.

Our study shows that BMP2 treatment improved angiogenesis and diabetic wound healing. Previously, topical growth factor therapy such as vascular endothelial growth factor (VEGF) has shown limited success in diabetic foot wounds. Although VEGF has displayed some angiogenic capacity, clinical trials have failed to show significant effects, leading to unsuccessful attempts in clinical settings.[7] Several factors, such as a short half-life, may have acted as a limiting factor that hinders its use in wound treatment. VEGF acts mainly on ECs and activation of angiogenesis.[15] BMP2 promotes activation and maturation of angiogenesis and affects not only ECs but also vascular smooth muscle cells.[15] Furthermore BMP2 stimulates dermal and epidermal growth, leading to keratinized and thickened skin.[40,54,59] In view of these points, since BMP2 acts on various cells necessary for wound healing, we propose that it is an excellent candidate for the treatment of chronic wounds.

This study had several limitations. First, the study subjects were limited to type 1 diabetes. Second, long-term side effects of BMP2 were not confirmed. However, BMP2 was approved by the FDA to use clinically, and it is not expected to have fatal side effects. BMP2 is an important molecule in causing vascular calcification by acting on vascular smooth muscle cells. Since microvessels were observed around wounds, BMP2 treatment does not appear to be related to cardiovascular pathology. However, for safety, long-term effects of BMP2 on wound sites need to be evaluated and validated through *in vivo* studies.

V. CONCLUSION

We designed LNP-PTD-BMP2, which possesses the ability to promote direct intracellular transduction and angiogenesis (Fig. 9). Based on the accelerated wound healing effects of LNP-PTD-BMP2 observed in this study, we propose that LNP-PTD-BMP2 is a potential therapeutic agent that can be used in the treatment of diabetic wounds.

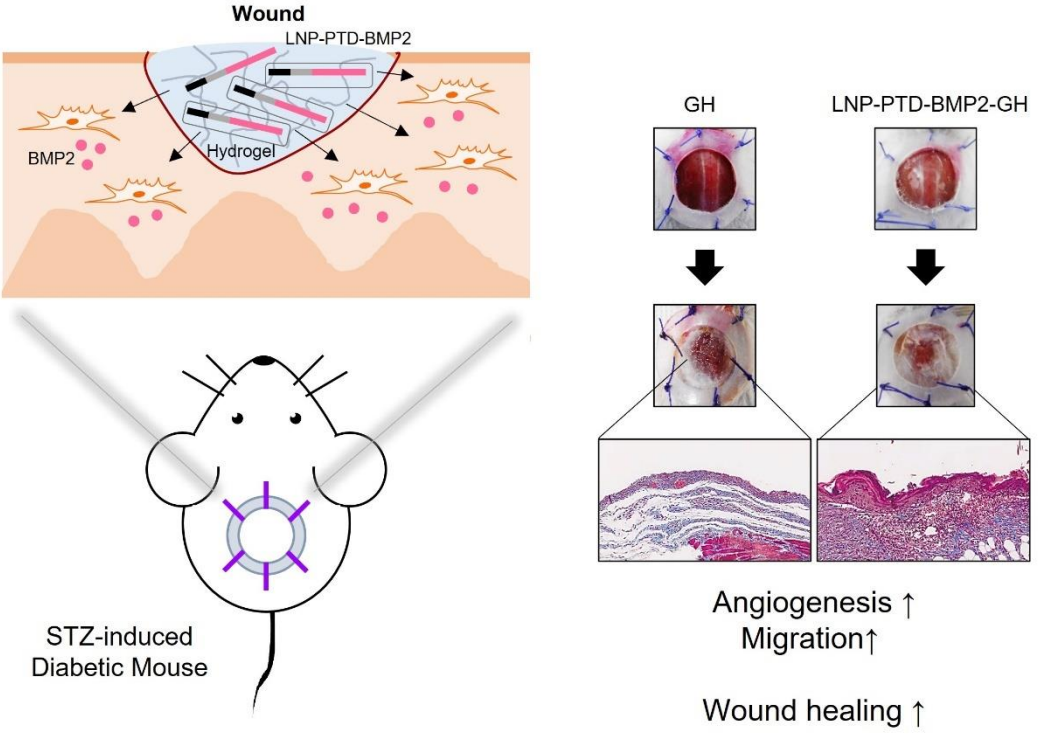

Figure 9. LNP-PTD-BMP2 is a potential therapeutic agent that can be used in the treatment of diabetic wounds.

REFERENCES

1. Wang X, Sng MK, Foo S, Chong HC, Lee WL, Tang MB, et al. Early controlled release of peroxisome proliferator-activated receptor β/δ agonist GW501516 improves diabetic wound healing through redox modulation of wound microenvironment. J Control Release 2015;197:138-47.
2. Yoon DS, Lee Y, Ryu HA, Jang Y, Lee KM, Choi Y, et al. Cell recruiting chemokine-loaded sprayable gelatin hydrogel dressings for diabetic wound healing. Acta Biomater 2016;38:59-68.
3. Baltzis D, Eleftheriadou I, Veves A. Pathogenesis and Treatment of Impaired Wound Healing in Diabetes Mellitus: New Insights. Advances in Therapy 2014;31:817-36.
4. Choi SM, Lee KM, Kim HJ, Park IK, Kang HJ, Shin HC, et al. Effects of structurally stabilized EGF and bFGF on wound healing in type I and type II diabetic mice. Acta Biomater 2018;66:325-34.
5. Singer AJ, Clark RA. Cutaneous wound healing. New England journal of medicine 1999;341:738-46.
6. Xu J, Zgheib C, Hu J, Wu W, Zhang L, Liechty KW. The role of microRNA-15b in the impaired angiogenesis in diabetic wounds. Wound Repair Regen 2014;22:671-7.
7. Okonkwo UA, DiPietro LA. Diabetes and Wound Angiogenesis. Int J Mol Sci 2017;18.
8. Ridiandries A, Tan JTM, Bursill CA. The Role of Chemokines in Wound Healing. Int J Mol Sci 2018;19.
9. Seo E, Lim JS, Jun JB, Choi W, Hong IS, Jun HS. Exendin-4 in combination with adipose-derived stem cells promotes angiogenesis and improves diabetic wound healing. J Transl Med 2017;15:35.
10. Galiano RD, Tepper OM, Pelo CR, Bhatt KA, Callaghan M, Bastidas N, et al. Topical Vascular Endothelial Growth Factor Accelerates Diabetic Wound Healing through Increased Angiogenesis and by Mobilizing and Recruiting Bone Marrow-Derived Cells. The American Journal of Pathology 2004;164:1935-47.
11. Kim NH, Cha YH, Kim HS, Lee SE, Huh JK, Kim JK, et al. A platform technique for growth factor delivery with novel mode of action. Biomaterials 2014;35:9888-96.
12. Benn A, Haupt J, Hildebrandt S, Kaehler C, Knaus P. Physiological and Pathological Consequences of Vascular BMP Signaling. In: Vukicevic S, Sampath KT, editors. Bone Morphogenetic Proteins: Systems Biology Regulators. Cham: Springer International Publishing; 2017. p.367-407.
13. Das A, Botchwey E. Evaluation of angiogenesis and osteogenesis. Tissue Eng Part B Rev 2011;17:403-14.
14. Raida M, Clement JH, Leek RD, Ameri K, Bicknell R, Niederwieser D, et al. Bone morphogenetic protein 2 (BMP-2) and induction of tumor

angiogenesis. J Cancer Res Clin Oncol 2005;131:741-50.
15. David L, Feige J-J, Bailly S. Emerging role of bone morphogenetic proteins in angiogenesis. Cytokine & growth factor reviews 2009;20:203-12.
16. Yoo SY, Kwon SM. Angiogenesis and its therapeutic opportunities. Mediators of inflammation 2013;2013:127170-.
17. de Jesus Perez VA, Alastalo T-P, Wu JC, Axelrod JD, Cooke JP, Amieva M, et al. Bone morphogenetic protein 2 induces pulmonary angiogenesis via Wnt–β-catenin and Wnt–RhoA–Rac1 pathways. 2009;184:83-99.
18. Langenfeld EM, Langenfeld J. Bone morphogenetic protein-2 stimulates angiogenesis in developing tumors. Mol Cancer Res 2004;2:141-9.
19. Rothhammer T, Bataille F, Spruss T, Eissner G, Bosserhoff AK. Functional implication of BMP4 expression on angiogenesis in malignant melanoma. Oncogene 2007;26:4158-70.
20. Finkenzeller G, Hager S, Stark GB. Effects of bone morphogenetic protein 2 on human umbilical vein endothelial cells. Microvasc Res 2012;84:81-5.
21. Woo EJ. Adverse events after recombinant human BMP2 in nonspinal orthopaedic procedures. Clinical orthopaedics and related research 2013;471:1707-11.
22. Evrard S, Delanaye P, Kamel S, Cristol J-P, Cavalier E, Arnaud J, et al. Vascular calcification: from pathophysiology to biomarkers. Clinica Chimica Acta 2015;438:401-14.
23. Peiffer BJ, Qi L, Ahmadi AR, Wang Y, Guo Z, Peng H, et al. Activation of BMP Signaling by FKBP12 Ligands Synergizes with Inhibition of CXCR4 to Accelerate Wound Healing. Cell Chem Biol 2019;26:652-61.e4.
24. Frankel AD, Pabo CO. Cellular uptake of the tat protein from human immunodeficiency virus. Cell 1988;55:1189-93.
25. Kim S, Shin DH, Nam BY, Kang HY, Park J, Wu M, et al. Newly designed Protein Transduction Domain (PTD)-mediated BMP-7 is a potential therapeutic for peritoneal fibrosis. J Cell Mol Med 2020; doi:10.1111/jcmm.15992.
26. Schwarze SR, Ho A, Vocero-Akbani A, Dowdy SF. In vivo protein transduction: delivery of a biologically active protein into the mouse. Science 1999;285:1569-72.
27. Kim S, Jeong CH, Song SH, Um JE, Kim HS, Yun JS, et al. Micellized Protein Transduction Domain-Bone Morphogenetic Protein-7 Efficiently Blocks Renal Fibrosis Via Inhibition of Transforming Growth Factor-Beta-Mediated Epithelial-Mesenchymal Transition. Front Pharmacol 2020;11:591275.
28. Kang M-L, Kim H-S, You J, Choi YS, Kwon B-J, Park CH, et al. Hydrogel cross-linking–programmed release of nitric oxide regulates

source-dependent angiogenic behaviors of human mesenchymal stem cell. Science Advances 2020;6:eaay5413.
29. Yang G, Xiao Z, Ren X, Long H, Qian H, Ma K, et al. Enzymatically crosslinked gelatin hydrogel promotes the proliferation of adipose tissue-derived stromal cells. PeerJ 2016;4:e2497-e.
30. Moreno-Bueno G, Peinado H, Molina P, Olmeda D, Cubillo E, Santos V, et al. The morphological and molecular features of the epithelial-to-mesenchymal transition. Nature Protocols 2009;4:1591-613.
31. Park YR, Sultan MT, Park HJ, Lee JM, Ju HW, Lee OJ, et al. NF-κB signaling is key in the wound healing processes of silk fibroin. Acta biomaterialia 2018;67:183-95.
32. Guo S, Lok J, Liu Y, Hayakawa K, Leung W, Xing C, et al. Assays to examine endothelial cell migration, tube formation, and gene expression profiles. Methods in molecular biology (Clifton, N.J.) 2014;1135:393-402.
33. Chung HW, Lim J-B. High-mobility group box-1 contributes tumor angiogenesis under interleukin-8 mediation during gastric cancer progression. Cancer science 2017;108:1594-601.
34. Kim C-K, Choi YK, Lee H, Ha K-S, Won M-H, Kwon Y-G, et al. The farnesyltransferase inhibitor LB42708 suppresses vascular endothelial growth factor-induced angiogenesis by inhibiting ras-dependent mitogen-activated protein kinase and phosphatidylinositol 3-kinase/Akt signal pathways. Molecular pharmacology 2010;78:142-50.
35. Baek Y-Y, Cho DH, Choe J, Lee H, Jeoung D, Ha K-S, et al. Extracellular taurine induces angiogenesis by activating ERK-, Akt-, and FAK-dependent signal pathways. European journal of pharmacology 2012;674:188-99.
36. Francescone RA, 3rd, Faibish M, Shao R. A Matrigel-based tube formation assay to assess the vasculogenic activity of tumor cells. J Vis Exp 2011; doi:10.3791/3040.
37. Yuan Y, Das SK, Li M. Vitamin D ameliorates impaired wound healing in streptozotocin-induced diabetic mice by suppressing NF-κB-mediated inflammatory genes. Bioscience reports 2018;38.
38. Deng Y, Han X, Yao Z, Sun Y, Yu J, Cai J, et al. PPARα agonist stimulated angiogenesis by improving endothelial precursor cell function via a NLRP3 inflammasome pathway. Cellular Physiology and Biochemistry 2017;42:2255-66.
39. Lee M, Han SH, Choi WJ, Chung KH, Lee JWJWR, Regeneration. Hyaluronic acid dressing (Healoderm) in the treatment of diabetic foot ulcer: a prospective, randomized, placebo-controlled, single-center study. 2016;24:581-8.
40. Moura J, Da Silva L, Cruz M, Carvalho E. Molecular and cellular mechanisms of bone morphogenetic proteins and activins in the skin:

potential benefits for wound healing. Arch Dermatol Res 2013;305:557-69.
41. Sieveking DP, Ng MKJVM. Cell therapies for therapeutic angiogenesis: back to the bench. 2009;14:153-66.
42. Kirana S, Stratmann B, Prante C, Prohaska W, Koerperich H, Lammers D, et al. Autologous stem cell therapy in the treatment of limb ischaemia induced chronic tissue ulcers of diabetic foot patients. 2012;66:384-93.
43. Berlanga-Acosta JJIwj. Diabetic lower extremity wounds: the rationale for growth factors-based infiltration treatment. 2011;8:612-20.
44. Shields LBE, Raque GH, Glassman SD, Campbell M, Vitaz T, Harpring J, et al. Adverse Effects Associated With High-Dose Recombinant Human Bone Morphogenetic Protein-2 Use in Anterior Cervical Spine Fusion. 2006;31:542-7.
45. Perri B, Cooper M, Lauryssen C, Anand NJTSJ. Adverse swelling associated with use of rh-BMP-2 in anterior cervical discectomy and fusion: a case study. 2007;7:235-9.
46. Tannoury CA, An HSJTSJ. Complications with the use of bone morphogenetic protein 2 (BMP-2) in spine surgery. 2014;14:552-9.
47. Botchkarev VAJJoID. Bone morphogenetic proteins and their antagonists in skin and hair follicle biology. 2003;120:36-47.
48. Li G, Cui Y, McILmurray L, Allen WE, Wang H. rhBMP-2, rhVEGF165, rhPTN and thrombin-related peptide, TP508 induce chemotaxis of human osteoblasts and microvascular endothelial cells. Journal of orthopaedic research 2005;23:680-5.
49. Machado RD, Aldred MA, James V, Harrison RE, Patel B, Schwalbe EC, et al. Mutations of the TGF-beta type II receptor BMPR2 in pulmonary arterial hypertension. Hum Mutat 2006;27:121-32.
50. Thomson JR, Machado RD, Pauciulo MW, Morgan NV, Humbert M, Elliott GC, et al. Sporadic primary pulmonary hypertension is associated with germline mutations of the gene encoding BMPR-II, a receptor member of the TGF-beta family. J Med Genet 2000;37:741-5.
51. Ma L, Chung WK. The genetic basis of pulmonary arterial hypertension. Hum Genet 2014;133:471-9.
52. Atkinson C, Stewart S, Upton PD, Machado R, Thomson JR, Trembath RC, et al. Primary pulmonary hypertension is associated with reduced pulmonary vascular expression of type II bone morphogenetic protein receptor. Circulation 2002;105:1672-8.
53. Morrell NW, Adnot S, Archer SL, Dupuis J, Lloyd Jones P, MacLean MR, et al. Cellular and molecular basis of pulmonary arterial hypertension. J Am Coll Cardiol 2009;54:S20-s31.
54. Hwang EA, Lee HB, Tark KC. Comparison of bone morphogenetic protein receptors expression in the fetal and adult skin. ymj 2009;42:581-6.

55. Lo KW-H, Ulery BD, Ashe KM, Laurencin CTJAddr. Studies of bone morphogenetic protein-based surgical repair. 2012;64:1277-91.
56. Lewis CJ, Mardaryev AN, Poterlowicz K, Sharova TY, Aziz A, Sharpe DT, et al. Bone Morphogenetic Protein Signaling Suppresses Wound-Induced Skin Repair by Inhibiting Keratinocyte Proliferation and Migration. Journal of Investigative Dermatology 2014;134:827-37.
57. Ahmed MI, Mardaryev AN, Lewis CJ, Sharov AA, Botchkareva NV. MicroRNA-21 is an important downstream component of BMP signalling in epidermal keratinocytes. Journal of cell science 2011;124:3399-404.
58. Sharov AA, Sharova TY, Mardaryev AN, di Vignano AT, Atoyan R, Weiner L, et al. Bone morphogenetic protein signaling regulates the size of hair follicles and modulates the expression of cell cycle-associated genes. 2006;103:18166-71.
59. François S, Eder V, Belmokhtar K, Machet M-C, Douay L, Gorin N-C, et al. Synergistic effect of human Bone Morphogenic Protein-2 and Mesenchymal Stromal Cells on chronic wounds through hypoxia-inducible factor-1 α induction. Scientific Reports 2017;7:4272.

ABSTRACT(IN KOREAN)

LNP 제형화된 단백질 전달 영역이 포함된 BMP2의 제1형 당뇨쥐 상처 치유 효과

<지도교수 이진우>

연세대학교 대학원 의학과

서 재 완

혈관신생능의 저하는 당뇨환자의 상처치유지연에서 중요한 병인으로 알려져 있다. 골형성 유도 물질로 FDA의 승인을 받은 재조합 골형성 단백질-2(rhBMP2)는 혈관신생에 작용하는 것으로 알려졌다. 그러나 rhBMP2는 짧은 반감기 등의 제한점으로 상처치유에 적용하는 데 어려움이 있다. rhBMP2와 같은 수용성 성장인자들의 제한점을 해결하기 위해서 LNP(지질나노입자, lipid nanoparticle) 제형화된 단백질 전달 영역(protein transduction domain, PTD)을 활용한 새로운 전달 모형이 활용됐다. 본 연구의 목적은 LNP 제형화된 PTD-BMP2 (LNP-PTD-BMP2)를 gelatin hydrogel(GH) 드레싱을 사용하여 당뇨병성 상처에 적용하였을 때 LNP-PTD-BMP2가 성공적으로 세포내로 transduction할 수 있는지 여부와 BMP2의 혈관신생 기능이 당뇨병성 상처치유를 향상시키는지를 확인하는 것이다.

In vitro에서 시행한 혈관신생연구에서 LNP-PTD-BMP2는 인간제대정맥내피세포(HUVEC)의 더 높은 튜브 형성을 유도하였고, scratch wound assay에서 LNP-PTD-BMP2는 대조군, rhBMP2보다 인간각질형성세포(HaCaT)의 더 많은 세포 모집 능력(cell recruitment capacity)을 유도했다. In vivo에서 streptozotocin으로 유도한 당뇨쥐의 등에 전층피부상처를 낸 후 microbial transglutaminase로 crosslink한 GH에 대조군, rhBMP2, LNP-PTD-BMP2를 각각 넣어 적용하였다. LNP-PTD-BMP2로 처치한 상처에서 유의하게 빠른 상처치유율 및 재상피화율과 유의하게 높은 collagen 침착이 관찰되었다. 면역형광염색분석에서 LNP-PTD-BMP2로 처치한 상처에서 CD31과 α-SMA 양성 세포 수가 유의하게 증가하여 신생혈관형성능력이 향상된 것을 확인하였다. 또한, in vivo 근적외선형광영상분석에서는 LNP-PTD-BMP2가 rhBMP2보다 반감기가 더 길고 BMP2 방출 영역이 상처 주위에 국한됨을 확인하였다. LNP-PTD-BMP2는 당뇨상처에 성공적으로 transduction되었고 혈관신생 및 상처치유를 향상시켰다. 본 결과들을 종합할 때, LNP-PTD-BMP2는 당뇨병성 상처치료에 잠재적인 치료제로 생각한다.

핵심되는 말: 당뇨, 상처 치유, 혈관 신생, 지질나노입자, 단백질 전달 영역, 재조합 골형성 단백질-2, gelatin hydrogel